Annual Report 2014 - BASE Collaboration

S. Ulmer[1], C. Smorra[1,2], A. Mooser[1], K. Franke[1,4], T. Higuchi[5], H. Nagahama[1,5], G. Schneider[1,3], S. Van Gorp[6], K. Blaum[4], Y. Matsuda[5], C. Ospelkaus[7], W. Quint[8,9], J. Walz[3,10], and Y. Yamazaki[6]

[1] *RIKEN, Ulmer Initiative Research Unit, Wako, Saitama 351-0198, Japan*

[2] *CERN, CH-1211 Geneva, Switzerland*

[3] *Institut für Physik, Johannes Gutenberg-Universität D-55099 Mainz, Germany*

[4] *Max-Planck-Institut für Kernphysik, Saupfercheckweg 1, D-69117 Heidelberg, Germany*

[5] *Graduate School of Arts and Sciences, University of Tokyo, Tokyo 153-8902, Japan*

[6] *RIKEN, Atomic Physics Laboratory, Wako, Saitama 351-0198, Japan*

[7] *Leibniz Universität Hannover, D-30167 Hannover, Germany*

[8] *Ruprecht Karls-Universität Heidelberg, D-69047 Heidelberg, Germany*

[9] *GSI - Helmholtzzentrum für Schwerionenforschung, D-64291 Darmstadt, Germany and*

[10] *Helmholtz-Institut Mainz, D-55099 Mainz, Germany*

(Dated: January 7, 2015)

Abstract

BASE [1, 2] aims at direct high-precision measurements of the magnetic moments of the proton and the antiproton. This document reports on recent progress of BASE. Highlights are the first direct and most precise measurement of the magnetic moment of a single trapped proton [3], performed at our experiment at Mainz, as well as trapping and preparation of a single antiproton with the recently built experiment at CERN.

CERN-SPSC-2015-003 / SPSC-SR-152
07/01/2015

INTRODUCTION

CPT symmetry is the most fundamental discrete symmetry in the Standard Model of particle physics. As a consequence it is predicted that e. g. lifetimes, masses, charges, and magnetic moments of matter and antimatter equivalents are identical, aside from signs. CPT invariance is, however, in strong contradiction to the observed matter/antimatter imbalance in our Universe, and its reason has yet to be understood. This inspires experiments to compare the fundamental properties of matter and antimatter with great precision. E.g. in oscillation experiments the masses of K-mesons were compared with a fractional precision at the 10^{-18} level [5]. In the lepton sector the continuous Stern Gerlach effect in Penning traps was used to compare the $g-2$ values of electron and positron with a fractional precision of 3.5 ppt [6]. By applying similar measuring schemes, the magnetic moments of the proton and the antiproton were compared with a precision of 4.4 ppm [7]. BASE is planning to improve this comparison by at least a factor of 1000 to provide one of the most sensitive tests of CPT invariance in the baryon sector.

MEASUREMENTS AT BASE-MAINZ

To achieve the goal of performing the above direct high-precision measurements, the double Penning trap [8] technique will be used. As progress towards the application of this method we demonstrated

- the first observation of spin flips with a single trapped proton [9] using statistical spin-flip detection,
- a precision measurement of the magnetic moment of the proton at the ppm level [10],
- the first direct observation of single spin flips with a single proton [11],
- the demonstration of the double Penning trap technique with a single proton [12].

Within 2014 we realized the last step, and measured the proton magnetic moment with the double-trap method [3]. A fractional precision of 3.3 ppb was achieved. Our measurement is 760 times more precise than achieved in previous Penning trap experiments [13], outperforms the 1972 maser measurement [14] by a factor of 3, and improves the currently accepted

literature value by a factor of 2.5 [15], which is illustrated in Fig. reffig:Measurements. With these developments we have the methods at hand to improve the precision of the magnetic moment of the antiproton by more than a factor of 1000.

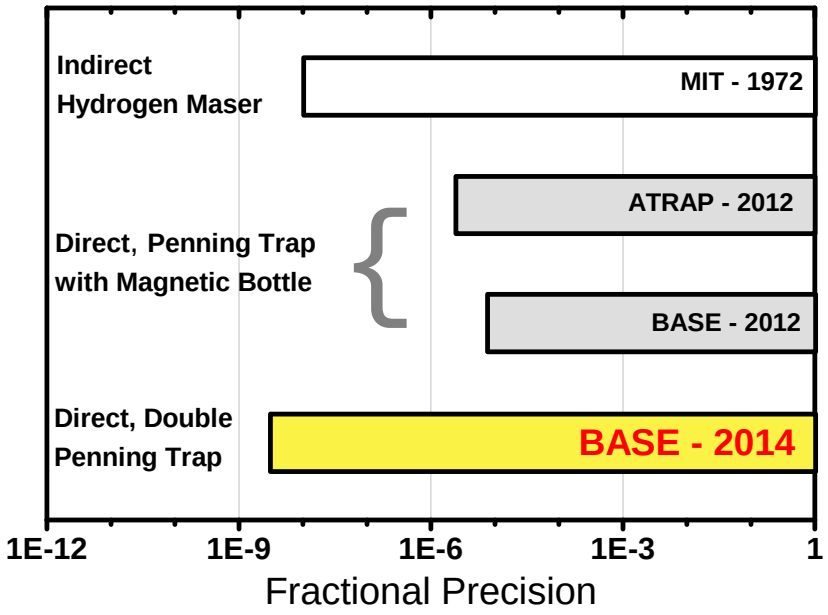

FIG. 1. Relative precision achieved in measurements of the proton magnetic moment. The value extracted indirectly from measurements with a hydrogen maser has a precision of 10 ppb. Direct measurements with a single proton in a Penning trap with strong superimposed magnetic inhomogeneities were performed in 2012 by us and a group at Harvard. The result of the measurement described in [3] was achieved by using the double Penning-trap technique with a single trapped proton. Our result is about 760 times more precise than other direct single particle measurements.

BASE AT CERN - CONTRIBUTIONS FROM CERN

To apply our techniques to the antiproton a new experiment has been set-up at CERN [2]. A dedicated experiment zone (DE5) and an antiproton transfer line were constructed, and implemented into the AD facility. An integration drawing is shown in Fig. 2.

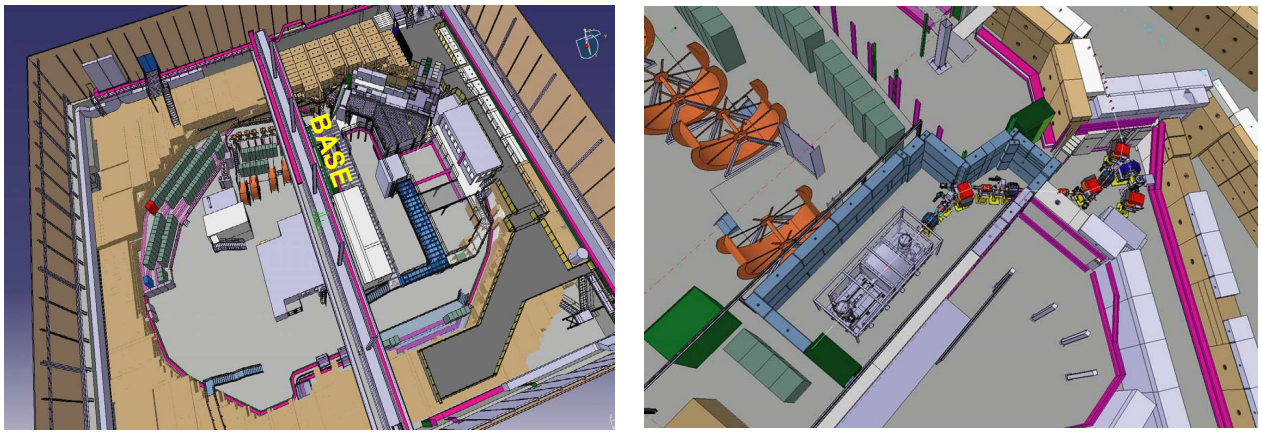

FIG. 2. Integration of BASE into the AD-facility. Left: Overview of the AD-hall, right: detailed view of the BASE experiment.

Experiment Zone

Integration work on the new experiment zone started in September 2013, the experiment space was provided in November 2013 and immediately afterwards the BASE team started installation of the experiment frame and a superconducting magnet.

Integration of Beamline Elements

A dedicated antiproton transfer-line was constructed by CERN [2]. Involved in the project were BE, EN-MME, Integration Service, vacuum group, magnet group, BTV group, and the beam stopper group of CERN. All beamline elements were delivered on schedule or with only marginal delays. Integration of the beamline elements (3 bending magnets, 3 quadrupoles, 3 corrector magnets, 3 BTV monitors) started by the end of April 2014. The installation of the elements was finished by the beginning of June 2014.

Beamline Vacuum Chambers and Implementation

Technical drawings for about 20 new vacuum chambers were provided by CERN-EN-MME department. All drawings were finished by the beginning of February 2014 and the production of the chambers started immediately afterwards. About 50% of the chambers were manufactured by the workshops of the BASE collaborating institutes (namely GSI

Darmstadt and MPIK Heidelberg). All beamline vacuum chambers, including special Y-chambers manufactured by the CERN workshop, were delivered by the beginning of June 2014. After cleaning and vacuum-testing of the chambers, these parts were implemented into the beamline magnets. All related integration work was finished by middle of July 2014. Within the following month cabling of the beamline elements took place. By the middle of August 2014 the installation of the BASE antiproton transfer line was considered as finished.

BASE AT CERN - EXPERIMENT

The BASE group at CERN was building a new Penning trap apparatus including an experiment frame, a supercounducting magnet, cryogenic mechanics, an advanced Penning trap system, detection electronics for all traps, high-voltage catching electronics, a robust degrader system, and a cryogenic beam monitor. Furthermore, advanced data recording and analysis techniques have been developed and implemented as a sound-card FFT/time transient recorder and an SQL based data-log system.

Magnet and Cryogenic Integration

Installation of an old superconducting magnet took place starting in the beginning of 2014. Due to strict CERN safety regulations the device had to be refurbished and equipped with state of the art safety devices. In parallel the cryogenic setup (two cryostats, thermal shields, support-mechanics for the trap) was assembled, tested, and tuned. The power consumption of the 77 K stage is at 20 W, the consumption of the 4 K stage at 150 mW. This allows us to operate the experiment for 5 days without any external cryoliquid supplies.

Degrader

Antiprotons from the AD are at 5.3 MeV and need to be further decelerated to be confined in the Penning trap system. To decelerate the antiprotons to energies which can be handled by the catching electrodes of the BASE apparatus (10 keV), thin degrader foils are used. Energetic antiprotons penetrate the degrader material and lose energy by Coulomb-scattering

processes. If the degrader foil is adequately chosen, low energy antiprotons are transmitted which can be trapped. For BASE we developed a three-element degrader, shown in Fig. 3.

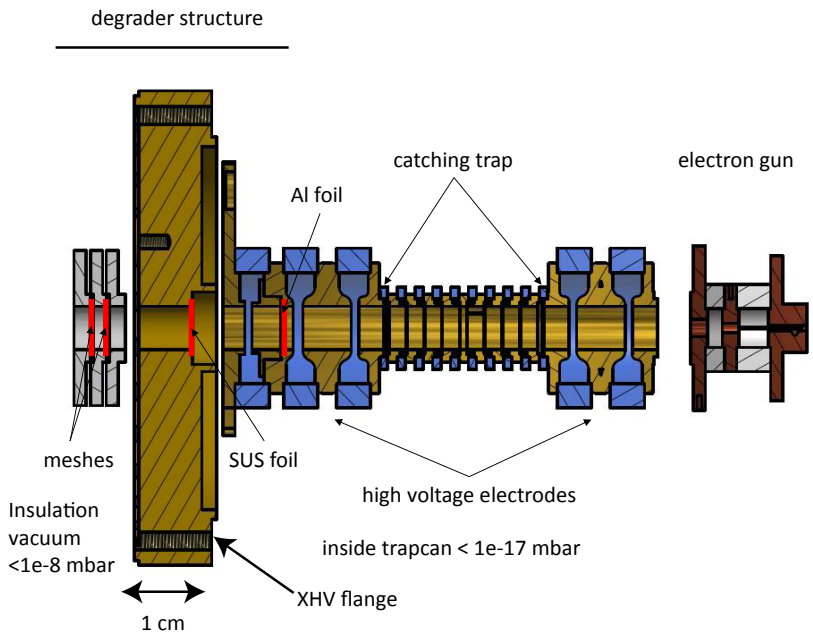

FIG. 3. Degrader structure used in BASE. For details, see text.

The most upstream element provides a variable stopping power to compensate uncertainties in stopping power calculations and material thicknesses. It consists of six stacked copper meshes with a thickness of 2.5 μm rotated by 15 degrees to each other. The grid structure of the mesh (15.6 μm, 44% open area) is much finer than the antiproton beam diameter, which is typically 2 mm at this position. This mesh assembly adds a large variety in stopping power in the range of 0 to 24 μm aluminium equivalent depending on the number of mesh holes passed by each antiproton. Compared to other degrader constructions this system provides lower transmission, however, it has remarkably robust acceptance. This degrader element is placed in front of the Penning-trap chamber. The second degrader is a window degrader which separates the insulation vacuum of about 10^{-8} mbar and the ultra-high vacuum of the hermetically-sealed Penning trap chamber. The window consists of a 25 μm stainless-steel foil which is hard-soldered into a flange closing the trap-can. The third element is an aluminum foil inside the trap-can, placed 5 cm away from the center of the catching trap. The purpose of this last foil is to match the total stopping power of to obtain the maximum number of slow antiprotons. According to simulations, this three-stage degrader system has

a catching efficiency better than 10^{-4} in a broad range around the optimum thickness.

Beam Monitor

To focus the beam to the center of the degrader a beam position monitor, operational in high vacuum (10^{-8} mbar), at ambient temperatures of 4 K and a magnetic field of 2 T was developed. It consists of four isolated copper plates on a PCB board and four low-noise cryogenic charge sensitive amplifiers see Fig. 4 a) and b).

Antiprotons are detected destructively by their charge deposited after colliding with the

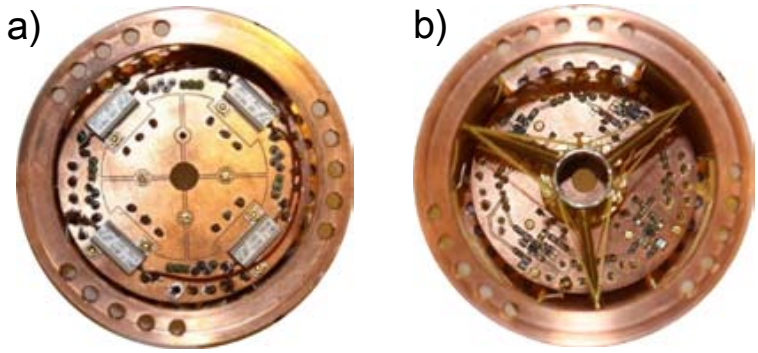

FIG. 4. Beam position monitor. a) shows the upper side of the monitor with its four triangular detection sufaces and four additional exernal heaters. b) shows the bottom side of the monitor with its four charge sensitive amplifiers and the kevlar mountig structure in yellow.

detector surfaces. With beam intensities of typically $3 \cdot 10^7$ antiprotons low signal strengths of about 3 pC are expected and amplification close to the signal source is needed. Thus, CMOS OP-amp based cryogenic charge sensitive amplifiers were built. Several silicon CMOS devices where tested with respect to robustness against thermal cycling, minimum operational temperature, slew rate and amplification. A combination of thermal decoupling using stainless steel supports and Kevlar fibers, as well as local heaters is used to mount the monitor to the 4 K stage. This allows for low-power heat-up of the amplifier stages above operation temperature (40 K). Self-heating at a power consumption of 2 mW is sufficient for continuous operation of the monitor. An amplification of 2.5 V/pC at temperatures of 40 K was achieved.

Soundcard FFT/Transient Analysis

The eigenmotions of particles trapped in a Penning trap can be modeled as series LC circuits. These short the thermal Johnson-Nyquist noise of the detection system resonator, creating a "dip" or notch in the measured noise spectrum at the eigenfrequency of the particle. Such noise spectra are typically mixed down to audio frequencies (≈10–20 kHz)

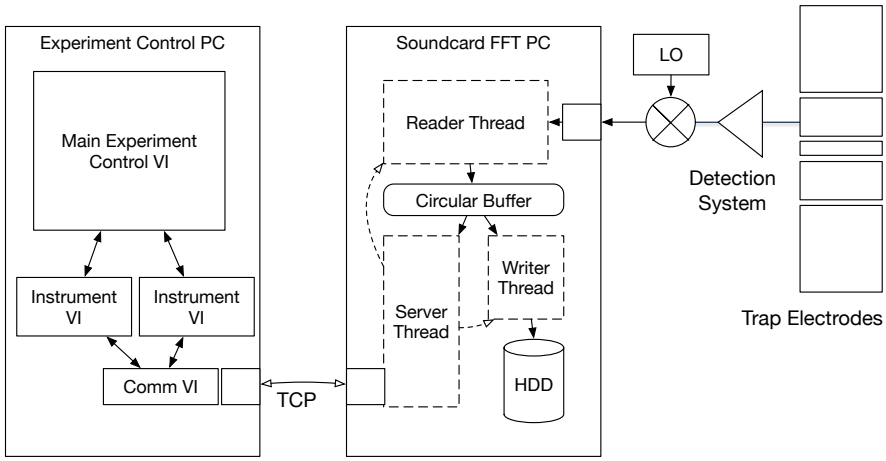

FIG. 5. Schematic of the acquisition software (center), the main experiment PC (left) and the detection system (right)

and recorded by an FFT-analyzer. However, these analyzers are not without shortcomings, since only the final transform can be saved, and the time-domain signal is lost. To address this issue, BASE produced a sound card based FFT analyzer/transient recorder (see figure 5). This is a piece of software, written in C, running on an SLC6 Linux PC. A recording thread continuously reads data from a high-quality sound card into a long circular memory buffer. A second thread optionally writes from this memory buffer to file storage for the recording of long (hours in length) transient files. Such data is useful for determining optimal measurement times. Finally, a server thread listens for and replies to TCP messages from the experiment controller PC. This PC runs NI LabView under Windows and controls the experiment. A collection of modular LabView VIs enable communication with the transient recorder. The FFT analyzer/transient recorder is integrated into the BASE control program.

SQL based Data-Log System

The data-logging system of BASE continuously records and stores the temperature of the apparatus, the temperature of the voltage supplies for the trap electrodes, ambient temperature of the AD hall, vibrations of the apparatus (using seismometers), as well as data obtained from an array of magnetic field sensors (Hall, Flux Gates and GMR sensors). The data are stored in an SQL database. Among the log information, the information of the magnetic field is the most important for the experiment. By that we can characterize external fluctuations caused by operation of the cranes in the AD hall, ramping of the magnets of other experiments, etc.. A GMR sensor is used to detect magnetic field fluctuations caused by the AD operations, which are typically in the order of 10 to 100 nT, see Fig. 6 shows the magnetic field fluctuation by AD operation detected by the GMR sensor. A detailed understanding of fluctuations caused by the AD is crucial for the planned precision measurements. This data-log system allows us to use any monitored external fluctuation as a trigger for cuts in data-evaluation.

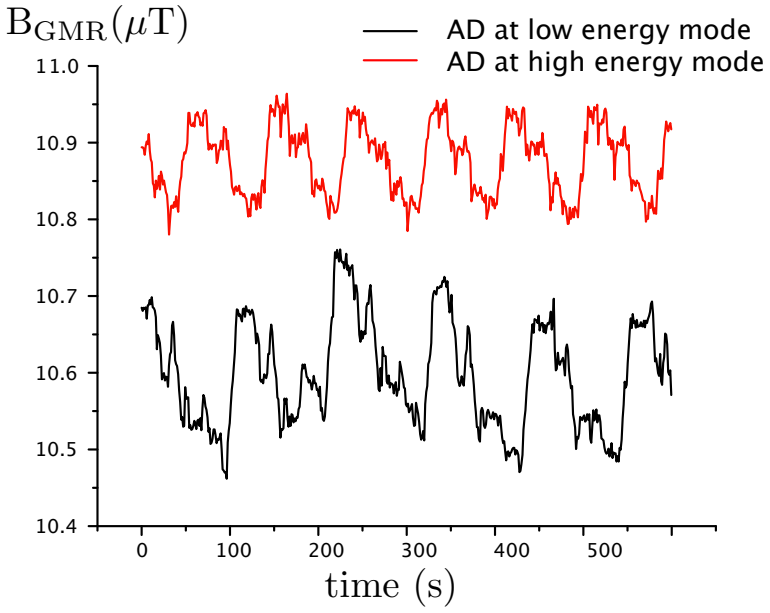

FIG. 6. Magnetic field fluctuations due to the AD operations. Oscillating fluctuations have cycles of 110 s for the low energy operation and 80 s for the high energy operation.

COMMISSIONING WITH PROTONS

To prepare for the antiproton physics run the experiment was commissioned with protons. This includes commissioning of the highly sensitive superconducting detection systems, four axial and two cyclotron detectors, preparation and cleaning of single protons, shuttling of particles inside the trap stack, detection of particles in different traps, as well as implementation of several basic ion trap techniques.

Detection Systems

Highly-sensitive superconducting detection systems, based on parallel tuned circuits and ultra low-noise amplifiers, are used to detect image currents induced in the Penning trap electrodes by single trapped particles [16]. BASE employs inductors made of superconducting Nb/Ti wire wound on PTFE cores (PTFE having an extremely low loss tangent at cryogenic temperatures) and selects amplifier transistors based on their effective gate resistance (among other parameters) [17]. The quality of a detection system is characterized by

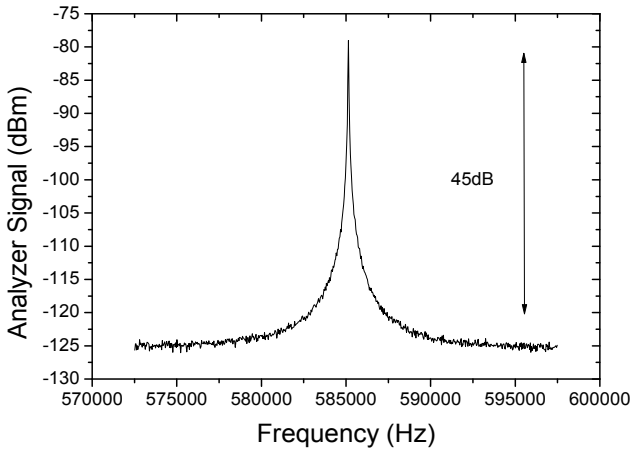

FIG. 7. Noise spectrum of one of the BASE axial detection systems. The quality factor is 25000 at a signal-to-noise ratio of about 45 dB. Frequency measurements with 15 mHz resolution are possible in an averaging time of 60 s.

its sensitivity

$$S \propto \sqrt{Q \cdot \sqrt{\mathrm{SNR}}}, \tag{1}$$

where Q and SNR are the quality factor of the detection system and the signal-to-noise ratio of the detector, respectively. Connected to the trap the BASE axial detection systems have quality factors on the order of 10 000 to 30 000 and signal-to-noise ratios up to 45 dB (see Fig. 7). This allows for frequency measurements with 15 mHz resolution in a typical averaging time of 60 s.

The superconducting cyclotron detection systems [17] have Q-values of between 1000 and 2000 at resonance frequencies of about 29 MHz. The high Q-values allow for cooling times on the order of 5 s to 10 s. Compared to the detectors used at the BASE companion experiment at Mainz both types of detection systems were significantly improved, allowing for faster g-factor measurement cycles in the CERN experiment. Our experiment at Mainz profits from these new developments, currently the detectors at Mainz are upgraded to prepare this apparatus for a measurement at the level of 100 ppt or better.

Preparation of Single Protons

Protons are created by bombarding a target with an electron beam. A part of the thereby evaporated hydrogen atoms is ionized by electron impact, and remaining protons are stored in the center of the trap. By sweeping the trapping voltages the content of the trap was analyzed and methods such as SWIFT cleaning combined with steep notch filtering were developed to clean the trap from contaminating ions. Further standard ion trap techniques were developed and experiment routines were implemented into the remote control system, as

- particle reduction techniques,
- preparation of single protons,
- harmonicity tuning of the trapping potential,
- adiabatic shuttling of the particles along the Penning trap stack,
- routines for precise frequency measurements.

Figure 8 shows FFT-spectra of a single trapped proton tuned to resonance of our reservoir trap detection system a.) and our precision trap detection system b.).

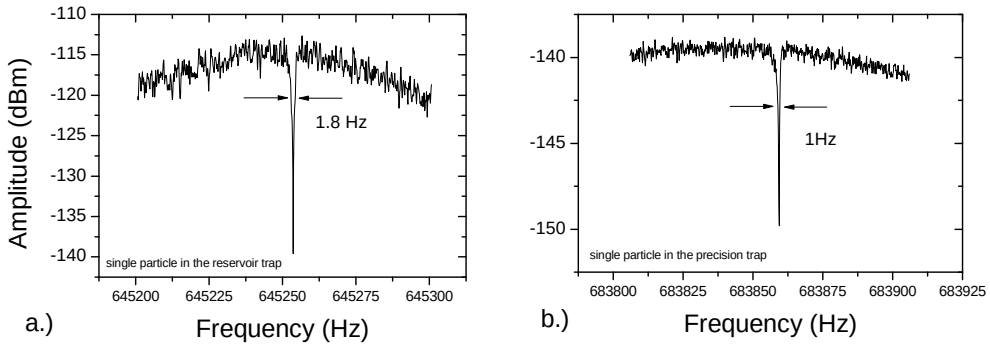

FIG. 8. Noise spectra of axial detection systems with a single proton tuned to resonance, a.) reservoir trap, b.) precision trap.

Although the trap geometry is identical for these two traps, the single particle dip linewidth $\Delta\nu_z$ is 1.8 Hz in the RT and about 1.0 Hz in the PT, which is due to different detector tuning. The PT detector is deliberately tuned to low damping, which leads to small dip-widths, thus enabling frequency measurements at higher precision within identical averaging time, since frequency resolution scales as $\sqrt{\Delta\nu_z}$.

SAFETY CLEARANCE

After the successful commissioning run with protons and a few upgrades of the experiment zone, BASE received safety clearance. HSE commented:

"...we recently finalized a very extensive safety clearance procedure for BASE. We just released the Memorandum DGS/SEE Safety clearance - Conventional Safety aspects for BASE, granting Safety Clearance for the operation of the 2014 BASE experimental run. We indeed reached the objective with a very productive collaboration between the HSE Unit, PH Safety Officers and the BASE GLIMOS. I would like to thank BASE for the huge effort in finalizing all the Safety checks asked, within the deadlines."

A time-line which summarizes the milestones achieved during the 2014 preparation work is shown in Fig. 9. To summarize the preparation work Fig. 10 shows photographs of the installed beamline and the operational BASE setup.

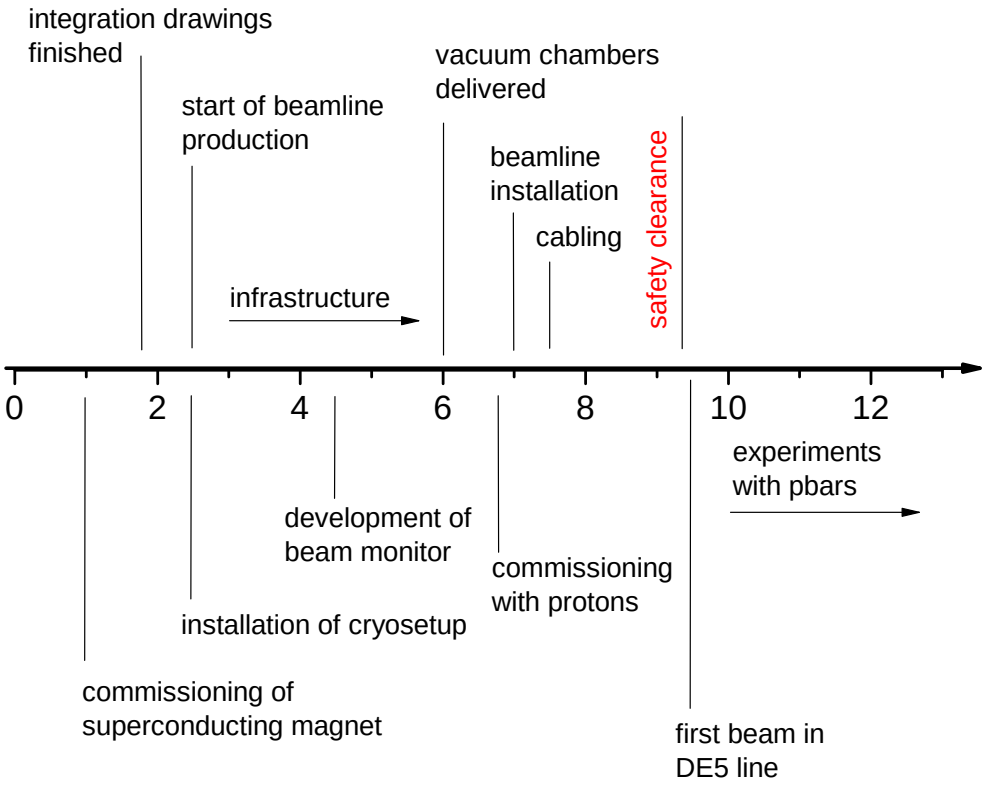

FIG. 9. Milestones achieved during the 2014 preparation work. (Time axis -¿ month)

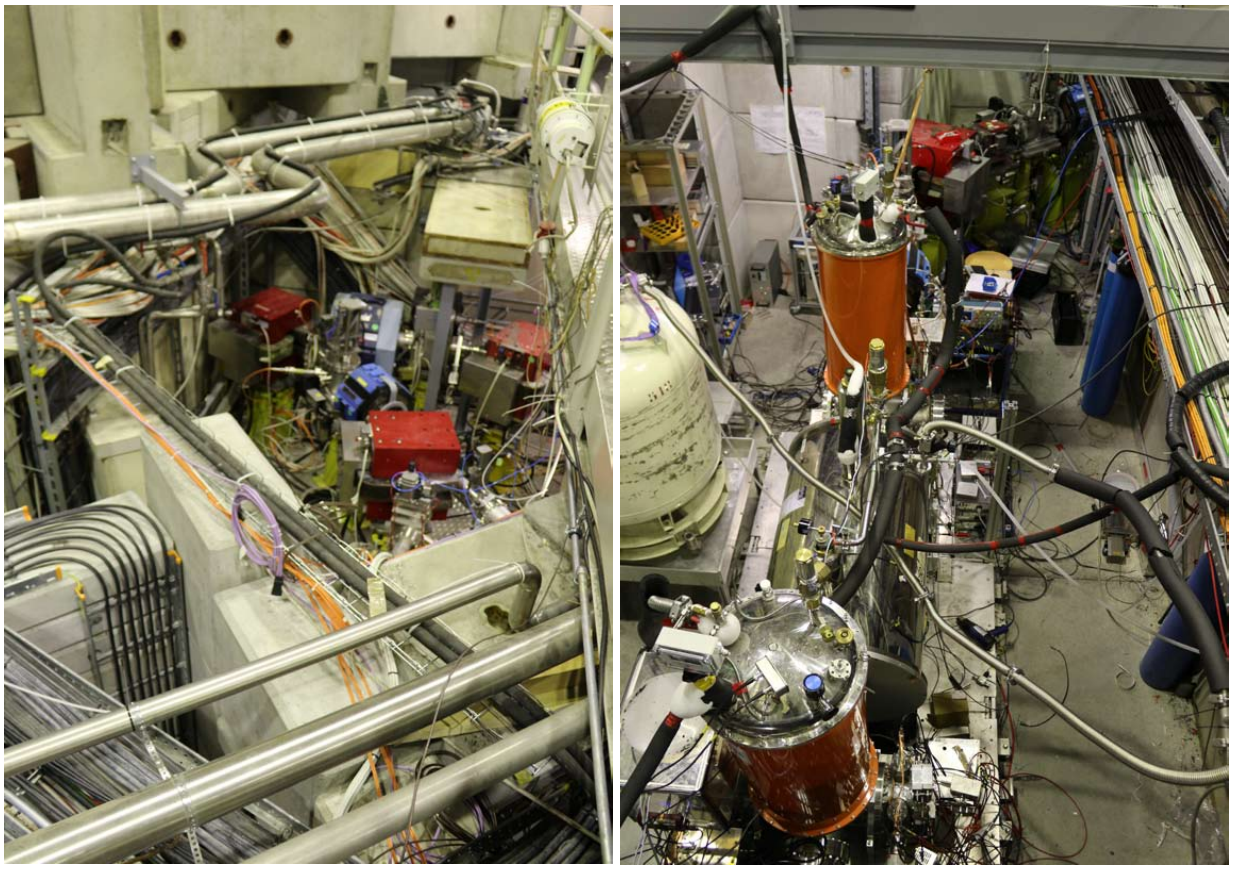

FIG. 10. Left: Upstream part of the DE5 line. Right: Downstream part of the DE5 line and BASE experiment.

ANTIPROTON PHYSICS RUN 2014

Commissioning of the DE5 Line

BASE was prepared to take the first antiproton bunches provided by the AD in 2014. Already the first extracted antiprotons were detected on the upstream BTV detector (DE5.BTV10). Thanks to the strong support of Lajos Bojtar it took only three shifts to commission the new DE5 line. Having fixed some minor polarity problems, an antiproton signal was detected on the BTV detector in front of the apparatus (see Fig. 11, left) and one shift later on the BASE beam monitor (see Fig. 11, right).

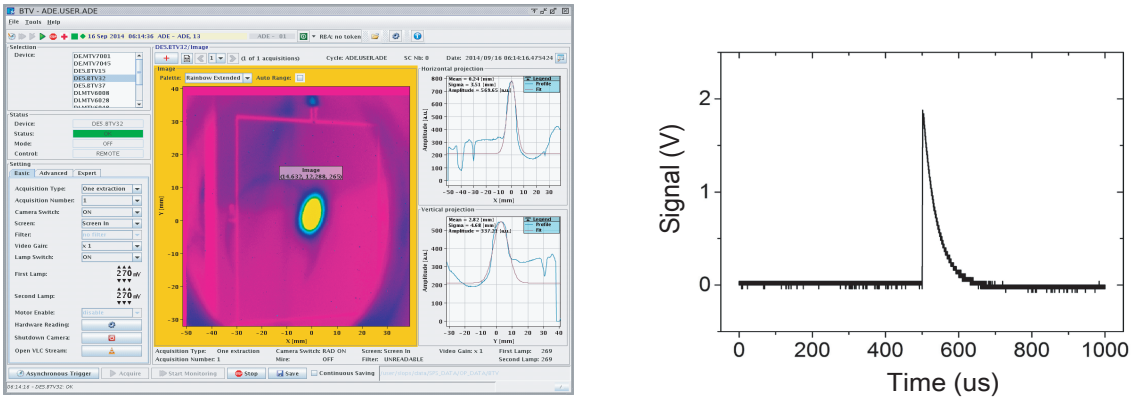

FIG. 11. Left: Screenshot of the BTV screen located upstream of the BASE apparatus. Right: antiproton charge-pulse on the BASE beam monitor.

First Trapped Antiprotons

Trapping of antiprotons was demonstrated in the following shift. Particles were trapped by an adequately timed 1 kV high-voltage pulse. After a certain waiting time the trap was opened, thereby antiprotons escaped from the trap and annihilated on the degrader. The extraction pulse triggered a scintillation detector placed close to our superconducting magnet and charged pions produced by the antiproton annihilation were detected unambiguously. The signal of the first detected annihilating antiprotons is shown in Fig. 12. From a rough calibration of the scintillator signal a catching efficiency of $\approx 10^{-4}$ (3000 antiprotons per

AD pulse) is extracted, which is consistent with the design values of our degrader system.

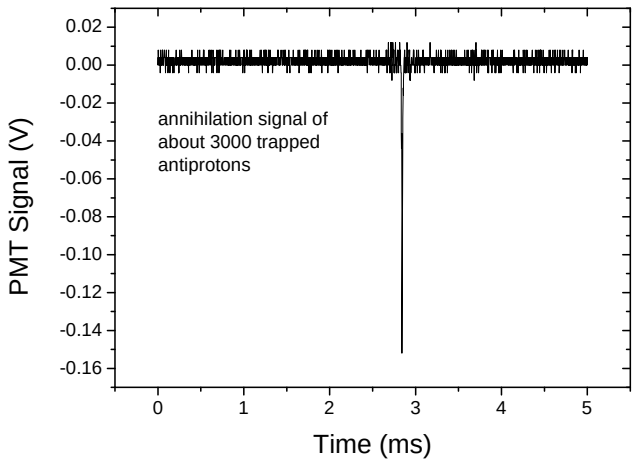

FIG. 12. Annihilation signal of trapped antiprotons which were first caught, stored for 20 seconds, and then released from the reservoir trap.

Electron Cooling and Electron Kickout

To reduce the keV axial energy further, about 10 000 electrons provided by a field emission electron source are loaded into the trap. Caught antiprotons interact with the particles by Coulomb collision and thermalize to the electron equilibrium temperature [18]. After thermalization electrons are heated out of the trap by strong axial rf-drives at the electron's axial oscillation frequency. This efficiently removes electrons from the center of the trap. However, e^- at high radii have significantly higher oscillation frequencies and are not affected by the drives. Thus the well-known electron kick-out scheme was prepared , which uses different oscillation time-scales due to the different inertial masses of electrons and co-trapped antiprotons. Schemes were established to move the cloud of electron-cooled trapped antiprotons to an electrode with small filter-time constant (biased by a diode-bridge filter). The particles were elevated and a kickout pulse was applied which opened the trap for 500 ns. Afterward the particles were transported back to the trap and the oscillation modes were cooled resistively. This scheme was applied for multiple times to ensure that no electrons remain in the trap.

Further Trap Cleaning

It turned out that the axial frequency was less stable than expected from stability measurements of the electrode biasing power supply voltage. This is a signature of additional trapped negative ions. Thus we tune the antiproton's resonance frequency to the center of a steep notch filter and apply a strong SWIFT drive in the frequency band 20 kHz to 550 kHz. Afterwards the trap potential is lowered and hot particles are evaporated. Finally we drive the modified cyclotron frequency of negative hydrogen ions and lower the trapping voltage again. Having repeated this scheme multiple times, the axial frequency stability is as expected, thus indicating a clean trap.

Resonant Detection

To detect the trapped antiprotons resonantly, parametric resonance was used. This is an elegant scheme to detect particles without detector saturation. In the scheme a drive at $2\nu_z$ was used and the trap voltage was adjusted to maximize the signal observed on the detector. The signal shown in Fig. 13 is the result of such a parametric excitation experiment. The clear peak on the center of the detector is due to antiprotons dissipating power on the detection resistor.

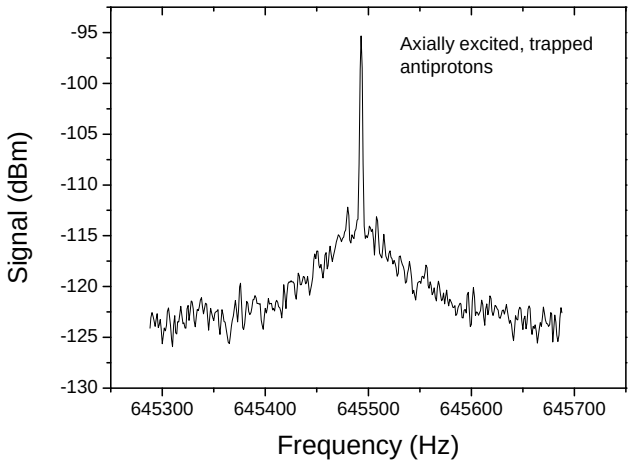

FIG. 13. Signal of parametrically excited antiprotons tuned to resonance with the reservoir trap detection system.

Dip Detection and Single Antiproton Preparation

Particles which are tuned to resonance with the detection system and cooled resistively to thermal equilibrium appear as a dip in the FFT spectrum of the detector. The width of the dip $\Delta\nu_z$ is a function of the number N of trapped particles

$$\Delta\nu_z = \frac{N}{2\pi\tau}, \tag{2}$$

where τ is the resistive cooling time constant of the detection system. Dip detection is an important experimental ingredient since it enables frequency measurements in thermal equilibrium, which is a crucial technique to perform high-precision g-factor measurements [3]. After applying the sequence of the above developed techniques together with sensitive tuning of the trapping potential allowed dip detection of trapped antiprotons. Figure 14

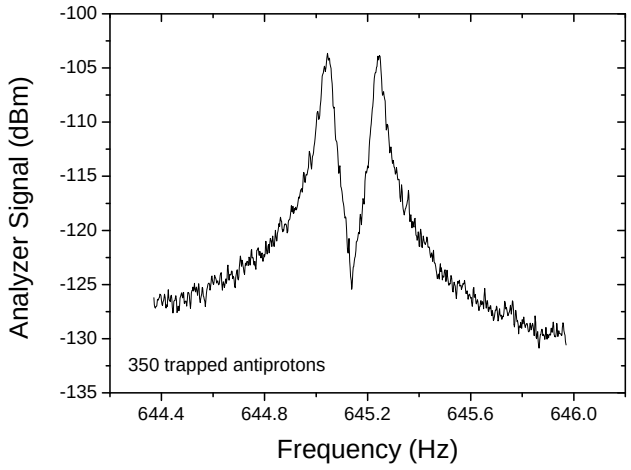

FIG. 14. Antiprotons cooled to thermal equilibrium with the axial detection system. The width of the dip in the noise-spectrum of the detector is proportional to the number of trapped particles. From a calibration we extract a number of about 350 trapped particles.

shows a dip signal produced by about 350 antiprotons caught in the BASE reservoir trap. To reduce the number of particles to one, resonant axial radio-frequency drives are applied and subsequently the trapping potential was lowered. By repeating this heating/dumping sequence, a single antiproton was prepared successfully. This is illustrated in Fig. 15. The FFT spectra show different amounts of antiprotons tuned in parallel to the detector. The figure on the lower right shows the width of the dip as a function of particle number. In the

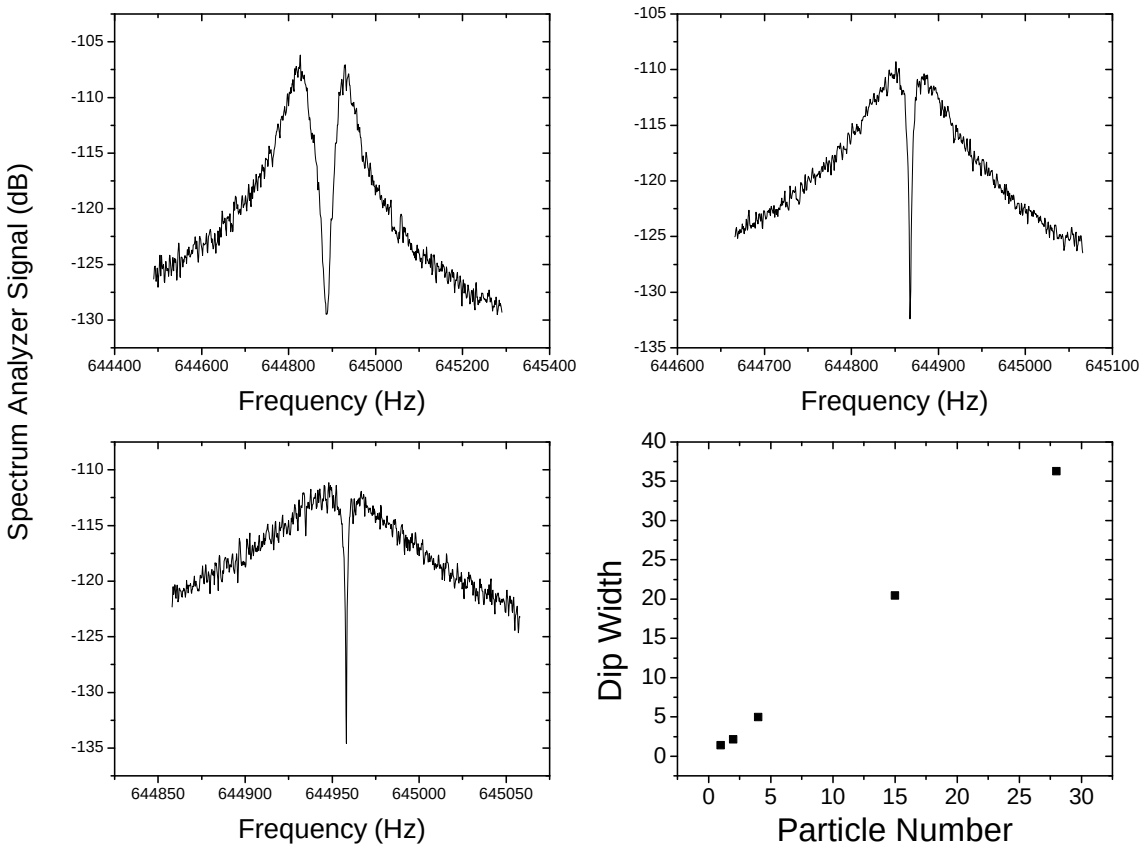

FIG. 15. Reduction of antiprotons. Upper: signal of different amounts of trapped antiprotons. Lower left: Single antiproton in the reservoir trap. Lower right: Line-width of the particle dip as a function of number of trapped particles.

reservoir trap a single antiproton has a line-width of 1.8 Hz.

In total it took 10 AD-shifts to establish all the techniques described above and to prepare a single antiproton in our trap system.

THE RESERVOIR TRAP

To operate BASE as well during the winter shutdown, when magnetic and radio-frequency noise in the AD-hall are low, we implemented a reservoir trap into our Penning-trap system, which is shown in Fig. 16. The idea is to load this trap with several AD shots and extract

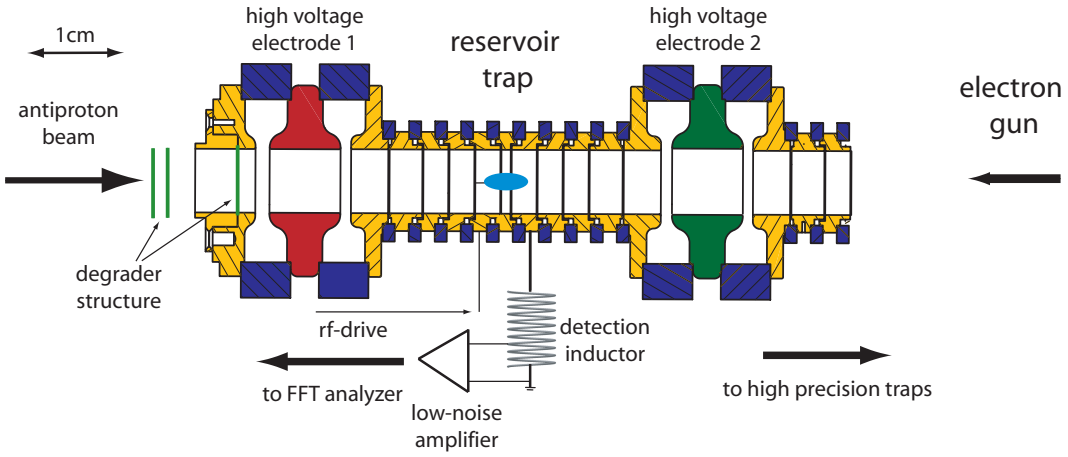

FIG. 16. BASE reservoir trap including all the crucial components used in the 2014 experiments.

single particles whenever a particle is lost in the precision experiment cycle. Having established the methods for antiproton catching and single particle preparation we focussed on the development of techniques which allow lossless extraction of a single antiproton into the precision Penning trap cycle.

Particle Extraction from the Reservoir

Several schemes were developed to extract single antiprotons from the reservoir. The most efficient is to use adiabatic potential ramps together with potential asymmetries which are deliberately applied to the correction electrodes of the trap. This is illustrated in Fig. 17. First, a cloud of cold antiprotons is prepared in the trap center (Fig. 17 *a.*)). Subsequently an asymmetric trapping potential is applied (Fig. 17 *b.*)) and the central ring electrode is ramped to negative voltages (Fig. 17 *c.*)). This ramp separates the particles into two fractions. One fraction is kept in the trap, while the other fraction is shuttled to the another trap (Fig. 17 *d.*) and *e.*)). The fraction of particles which is kept in the trap can be tuned sensitively by applying adequate potential asymmetries shifting the center of the cloud of trapped particles

before the separation ramp is applied. The separated fraction of a cloud of initially trapped

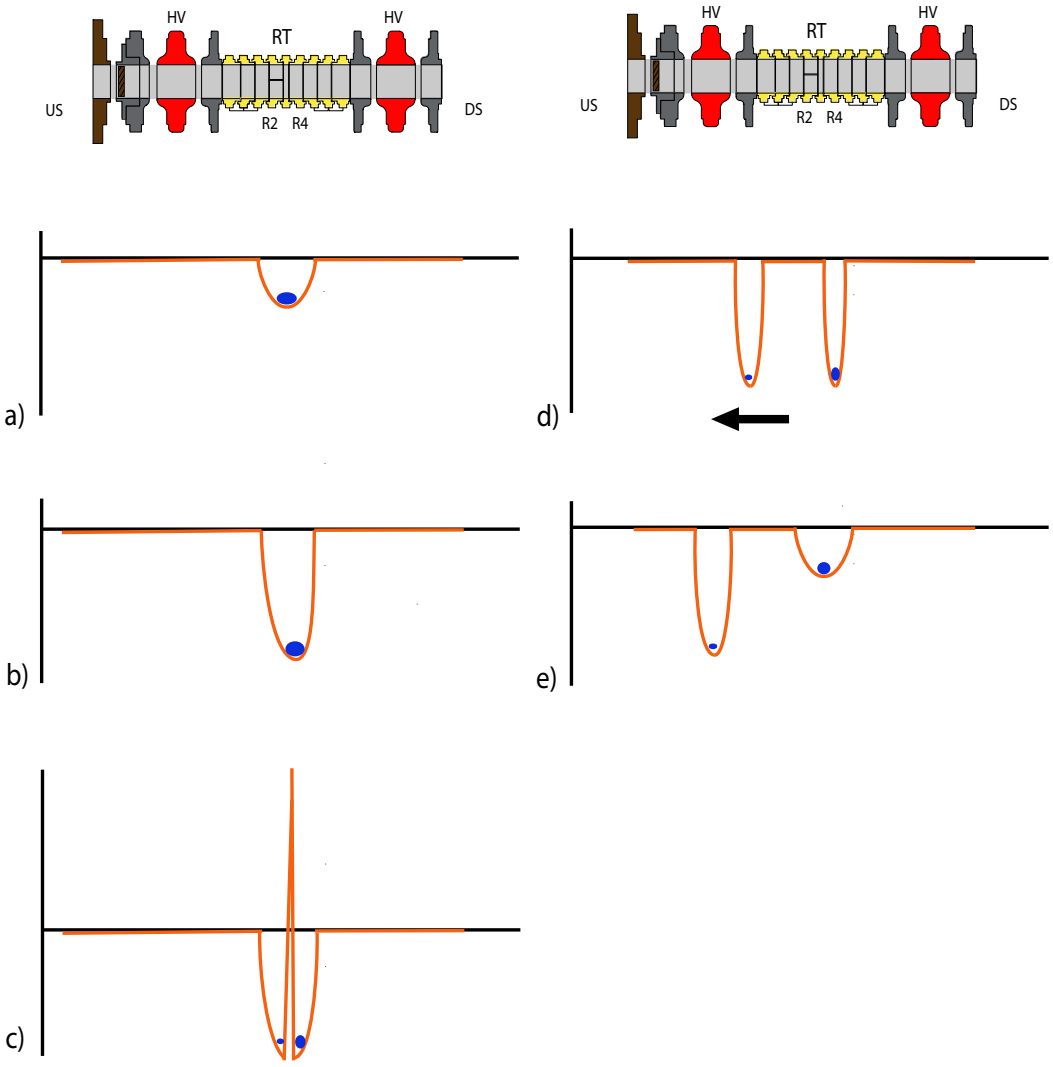

FIG. 17. Illustration of the developed particle separation scheme applied in the BASE reservoir trap. A detailed description is given in the text.

particles as a function of the applied asymmetry is shown in Fig. 18. The black squares represent the fraction which was parked upstream of the trap-center while the red circles represent the complement. With an appropriately tuned asymmetry it is even possible to extract fractions at the percent-level from the reservoir.

To extract a single particle the trap is tuned to high asymmetry, and the above scheme is applied. Once a large number of particles is initially present in the reservoir, extraction of a single antiproton is rather unlikely. However, by applying the above scheme iteratively

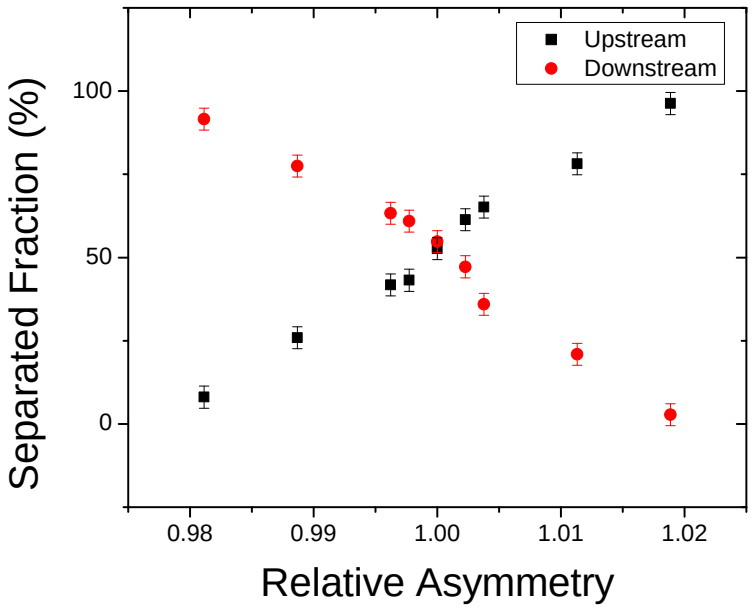

FIG. 18. Fraction of particles extracted from the reservoir as a function of the asymmetry applied in advance to the separation ramp.

single particle extraction is possible within a few steps. To this end, we first extract a small fraction of particles and keep it in the trap, while the larger fraction is parked in one of the other traps. Then a single particle is taken from the remaining fraction, which is then merged with the particle cloud parked in the other trap. By applying this scheme extraction of a single particle from a reservoir of about 100 antiprotons was demonstrated.
While performing experiments particles were lost from time to time, either deliberately, or due to human errors, never due to annihilation with residual gas atoms. In such a case the above extraction scheme was applied to reload the experiment cycle with a single antiproton. We took the last antiproton shot on the 27th of November 2014. Using the reservoir we were able to perform experiments until the 22nd of December 2014.

Particle Lifetime and Vacuum

Within the 2014 physics run only a few experiments to study the lifetime of the reservoir were performed. We trapped about 50 antiprotons in the RT and didn't observe any particle-loss in the reservoir within a trapping time of more than four weeks. With these observations

and using estimations developed by other groups enables us to set a limit of $< 5 \cdot 10^{-18}$ mbar for the pressure in our trap can. The corresponding background atom-density is comparable to that in the interstellar medium.

Lifetime of the trap

To survive power cuts, the trap, spectrum analyzers and control computers are operated on UPS supplies, which survive power cuts of up to 10 hours. In case of a power cut all gate valves are closed and the vacuum is cryo-pumped to a $5{\cdot}10^{-9}$ mbar vacuum, thus no additional pumping is required. We performed several test experiments simulating power cuts which confirmed the 10 hours lifetime. It was even possible to continue experiments while power was turned off.

SYSTEMATIC MEASUREMENTS

To prepare BASE for high-precision magnetic moment measurements, the rest of 2014 beamtime was mainly devoted to characterize and understand electrical and magnetic background fluctuations which are present in the AD-hall. While electrical noise is efficiently shielded and filtered by adequate radio-frequency shielding techniques and by using 5th order high-impedance filter stages, it turned out that magnetic field noise is a serious issue. In order to characterize magnetic field noise measurements of the cyclotron frequency were performed.

Swapping

For precise tests of CPT invariance we aim at comparisons of the properties of the proton and the antiproton, measured in the same apparatus. Thus we developed methods to interchange particles between a parking trap and a measurement trap. In the test experiments we prepared two antiprotons, each in a separate trap (see Fig. 19). It is important to note that the particles were prepared from different trap loading cycles. Using adiabatic potential ramps we interchanged the particles multiple times without losing them. The swapping time is 18 s. This will allow quasi-simultaneous measurements of the magnetic moments of the

proton and the antiproton. Our power supply geometry is designed in a way that loss-less polarity switching is possible.

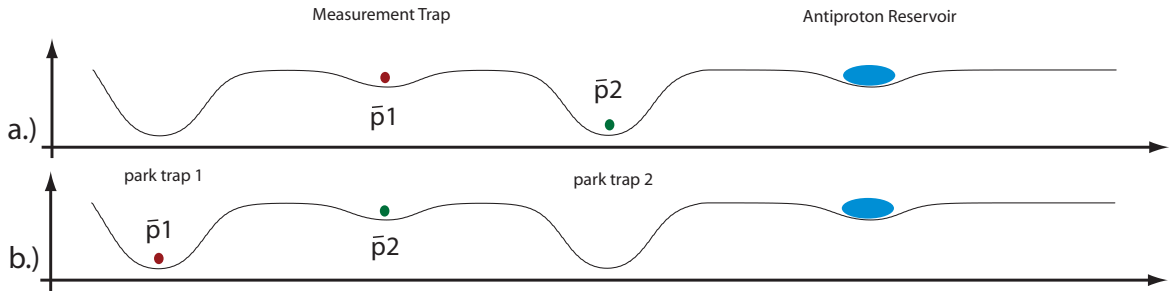

FIG. 19. Schematic illustrating the swapping experiments. a.) antiproton 1 is in the center of the measurement trap, antiproton 2 is parked in an electrode 5 cm downstream of the trap center, a reservoir of antiprotons is in a third trap. b.) antiproton 2 is in the center of the measurement trap, antiproton 1 is parked in an electrode 5 cm upstream of the trap center.

Feedback Cooling

An important technique in g-factor measurements is the application of feedback cooling. The signal of the detection system is phase shifted and fed-back capacitively, thus lowering effective particle temperature [19]. This narrows down the width of the g-factor resonance thus allowing for measurements at improved precision [20]. A feedback cooling circuit was implemented into the experiment and the technique was applied. In these experiments a single antiproton at a temperature of 2.5 K was prepared.

Cyclotron Frequency Measurements

The cyclotron frequency ν_c of a single particle in a magnetic field B is given by

$$\nu_c = \frac{1}{2\pi}\frac{q}{m}B, \tag{3}$$

where q/m is the particle's charge-to-mass ratio. Precise measurements of ν_c are crucial in high precision g-factor measurements which determine the magnetic moment of a particle in units of the nuclear magneton μ_N

$$\frac{g}{2} = \frac{\mu_{\bar{p}}}{\mu_N} = \frac{\nu_L}{\nu_c}, \tag{4}$$

where ν_L is the spin precession frequency. The cyclotron frequency of a single trapped particle is determined by measuring the particle's eigenfrequencies ν_+, ν_z and ν_- in the trap, and subsequent application of the invariance theorem [21]

$$\nu_c = \sqrt{\nu_+^2 + \nu_z^2 + \nu_-^2}. \tag{5}$$

We use sideband techniques to measure ν_+ and ν_- [22], the axial frequency is determined directly. Permanent frequency measurements together with independent magnetic field measurements by the sensor array, as well as pressure sensors, temperature sensors etc. were performed and evaluated to study magnetic field drifts caused by environmental changes. In un-triggered frequency measurements we observed beats between our measuring cycles and the AD deceleration cycle with amplitudes up of about 20 ppb and a period of 25 minutes. In addition, we observed pressure fluctuations in the LHe recovery line with amplitudes up to 20 mbars, which cause magnetic field shifts of several 100 ppb. Active stabilization of the LHe reservoir reduced the fluctuations by more than a factor of 100. Performing measurements with the pressure stabilized system and triggering of the measurement routine to the PS-to-AD injection, magnetic noise was reduced by a factor of 5.
By comparing the cyclotron frequency measurements to GMR sensor measurements frequency shifts caused by external magnet ramps, field drifts caused by crane operation etc. were identified (see Fig. 20). The plot shows in addition the rms-value of the shot-to-shot frequency fluctuation. Permanent steering of the ASACUSA beamline increases the frequency jitter from 160 mHz to 220 mHz. A fluctuation of 160 mHz is achieved in the ASACUSA back-shift while the AD is ramped in the background. This corresponds to a shot-to-shot fluctuation of 5 parts in a billion, and by that a similar line-width will be introduced in a g-factor measurement. However, appropriate averaging will enable BASE to measure much more precisely, and even with the current setup g-factor measurements at the level of 100 to 500 ppt will be possible.

Experiments after AD shutdown

AD-operation was stopped on the 15th of December 2014. Our long storage times enabled us to continue the 2014 BASE run until the 22nd of December, when the apparatus was heated up for several different reasons and the particles were deliberately kicked-out of

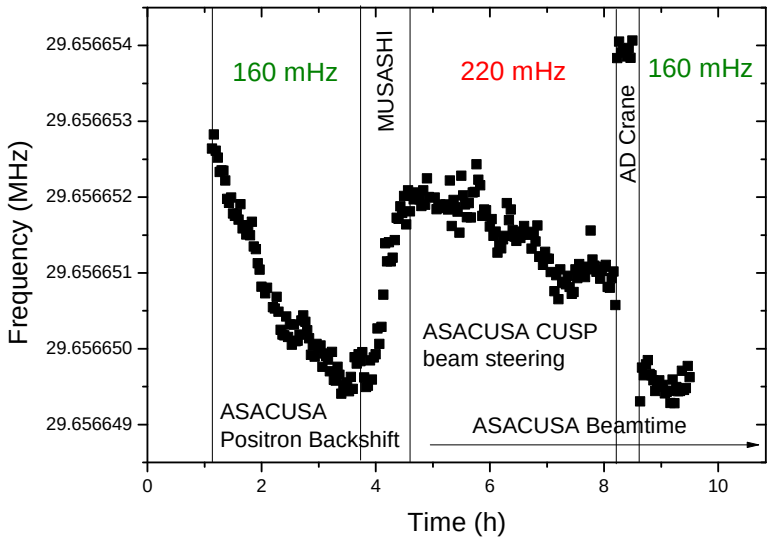

FIG. 20. Result of single antiproton cyclotron frequency measurements. Identified external drifts are labeled. The plot shows in addition the shot to shot fluctuation. Permanent steering of the ASACUSA beamline increases the frequency jitter from 160 mHz to 220 mHz. A 160 mHz fluctuation is achieved in the ASACUSA back-shift, when the AD-ring is operated in the background.

the trap. In this remaining week we continued our cyclotron frequency measurements. In these measurements the cyclotron frequency fluctuation was reduced by about a factor of 2. Without the significant fluctuations caused by AD operation we were able to determine the natural stability of our superconducting magnet, which is about 1.5 ppb per hour. A typical cyclotron frequency measurement takes at the moment about 100 s, thus, using phase sensitive methods [25, 26] it will be possible to perform cyclotron frequency measurements at the level of 50 ppt.

2015 WINTER SHUTDOWN AND FUTURE PERSPECTIVES

All above experiments were performed with an unshielded superconducting magnet. BASE ordered in April 2013 a state of the art magnet with a self-shielding factor > 100, which was only delivered in October 2014. During the winter shut-down 2015 the new device will be implemented into the BASE setup. In addition, a set of additional self-shielding coils will be prepared, which have the potential to contribute an additional self-shielding factor

of 50.

In addition to these mechanical modifications, phase-sensitive measurement techniques will be implemented and commissioning of the cooling trap and the spin-flip detection trap will be finished with protons to prepare BASE for a high-precision antiproton magnetic moment measurement in beamtime 2015.

ANTIPROTON BEAM CONSUMPTION

BASE is a single particle experiment which was specifically designed to consume only a minor amount of AD beam. To establish the methods described above we used three shifts for steering, two shifts to establish antiproton trapping, one shift to demonstrate electron cooling, two shifts to detect particles with our resonant detector, three shifts to commission electron kick-out schemes, one shift to prepare the antiproton dip, two shifts to demonstrate stacking, and one additional shift for further systematic studies, which are in total only 15 shifts. By using our antiproton reservoir we were able to continue experiments during the planned two weeks shut-down between the second and the third beamblock. The last antiproton shot was taken on the 27th of November 2014. With this last shot we managed to continue running the experiment until the 22nd of December 2014, when the apparatus was warmed up to exchange the superconducting magnet during the 2015 winter shutdown. The efficient development of the experimental methods enabled us to switch to parasitic mode already after the first week of the second beam-block. In this mode the AD-beam during BASE shifts was distributed/shared in a transparent way and in equal amounts among the other collaborations.

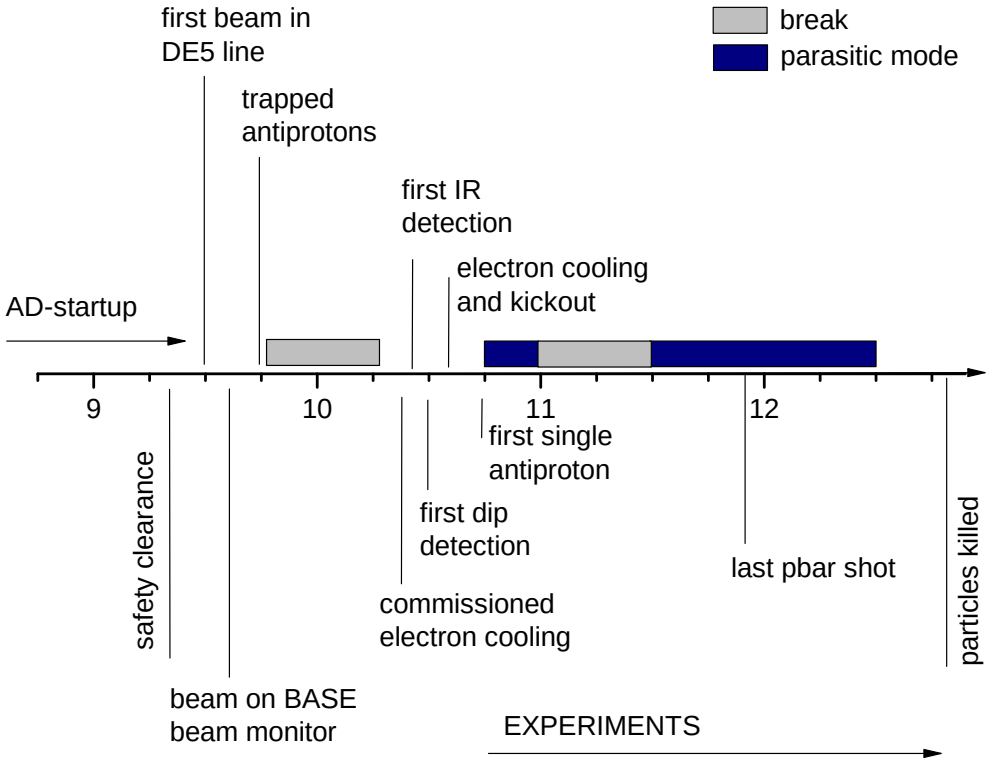

FIG. 21. Milestones achieved during the 2014 physics run.

CONCLUSION

In 2014 the BASE collaboration performed the first direct high-precision measurement of the magnetic moment of a single trapped proton with a fractional precision of 3.3 parts in a billion [3]. Our measurement is the most precise measurement of the proton magnetic moment to date, improving the currently accepted CODATA literature value by a factor of 2.5 [15]. In addition a new experiment was constructed and commissioned at the AD facility of CERN. We established crucial methods including antiproton trapping, electron cooling, electron kickout, and preparation of a single antiproton within a few shifts. In addition we commissioned our trap stack, and focused mainly on establishing schemes to use the reservoir trap as planned. In these experiments we developed techniques which allow loss-less extraction of a single antiproton from the reservoir, which can become a key technique for other precision experiments dealing with exotic particles. In addition we performed cyclotron frequency measurements with single trapped antiprotons, achieving shot-to-shot fluctuations at the level of 5 ppb in precision. These developments will enable g-factor measurements at a fractional precision of 500 ppt or better.

ACKNOWLEDGEMENT

We acknowledge support from the AD group, the engineering department, the vacuum-group, the rf-group, the integration service, the HSE department, the magnet group and the survey group of CERN. We would like to express our gratitude towards L. Bojtar for his coordinating work and his very strong support, as well as towards F. Butin for his strong support regarding integration of the experiment into the AD hall. We acknowledge financial support of RIKEN Initiative Research Unit Program, RIKEN President Funding, RIKEN Pioneering Project Funding, the Max-Planck Society, the BMBF, the Helmholtz-Gemeinschaft, HGS-HIRE, and the EU (ERC Advanced Grant No. 290870-MEFUCO and ERC Starting Grant No. 337154-QLEDS).

[1] S. Ulmer *et al.*, Letter of Intent, CERN document CERN-SPSC-2012-019 / SPSC-I-241 14/06/2012 (2012).

[2] S. Ulmer *et al.*, Technical Design Report, CERN document CERN-SPSC-2013-002 / SPSC-TDR-002 (2013).

[3] A. Mooser *et al.*, Nature **509**, 596 (2014).

[4] R. Bluhm, V. A. Kostellecky, and N. Russell, Phys. Rev. D **57**, 3932 (1998).

[5] F. Ambrosino *et al.*, [KLOE Collab.], JHEP **612**, 11 (2006) [arXiv:hep-ex/0610034].

[6] R. Van Dyck, Jr., P. B. Schwinberg and H. G. Dehmelt, Phy. Rev. Lett. **59**, 26 (1987).

[7] J. DiSciacca *et al.*, Phys. Rev. Lett. **110**, 130801 (2013).

[8] H. Häffner, T. Beier, S. Djekic, N. Hermanspahn, H.-J. Kluge, W. Quint, S. Stahl, J. Verdù, T. Valenzuela, and G. Werth, Eur. Phys. J. D **22**, 163 (2003).

[9] S. Ulmer, C. C. Rodegheri, K. Blaum, H. Kracke, A. Mooser, W. Quint, and J. Walz, Phys. Rev. Lett. **106**, 253001 (2011).

[10] C. C. Rodegheri, K. Blaum, H. Kracke, S. Kreim, A. Mooser, C. Mrozik, W. Quint, S. Ulmer, and J. Walz, Hyperfine Interact. **194**, 93 (2009).

[11] A. Mooser, H. Kracke, K. Blaum, C. C. Rodegheri, W. Quint, S. Ulmer and J. Walz, Phys. Rev. Lett. **110**, 140405 (2013).

[12] A. Mooser *et al.*, Phys. Lett. B **723**, 78 (2013).

[13] J. DiSciacca and G. Gabrielse, Phys. Rev. Lett. **108**, 153001 (2012).

[14] P. F Winkler, D. Kleppner, T. Myint, and F. G. Walther, Phys. Rev. A **5**, 83 (1972).

[15] S. G. Karshenboim and V. G. Ivanov, Phys. Lett. B **566**, 27 (2003).

[16] S. Ulmer, H. Kracke, K. Blaum, S. Kreim, A. Mooser, W. Quint, C. C. Rodegheri, and J. Walz, Rev. Sci. Inst. **80**, 123302 (2009).

[17] S. Ulmer *et al.*, Nucl. Instrum. Meth. A **705**, 55 (2013).

[18] G. Gabrielse *et al.*, Phys. Rev. Lett. **63** 1360 (1989).

[19] B. d'Urso, B. Odom, and G. Gabrielse, Phys. Rev. Lett **90**, 43001 (2003).

[20] L. S. Brown, Ann. Phys. **159**, 62 (1985).

[21] L.S. Brown and G. Gabrielse, Rev. Mod. Phys. **58**, 233 (1986).

[22] E. A. Cornell, R. M.Weisskoff, K. R. Boyce, and D. E.Pritchard, Phys. Rev. A, **41**, 312 (1990).

[23] G. Gabrielse, L. Haarsma, and S. L. Rolston, Int. J. Mass Spec. **88**, 319 (1989).

[24] S. Ulmer *et al.*, Phys. Rev. Lett. **107**, 103002 (2011).

[25] S. Rainville *et al.*, Nature **438**, 1096 (2005).

[26] S. Sturm et al., Phys. Rev. A **87**, 030501(R) (2013).